BOUNDARY LAYER COMBUSTION FOR VISCOUS DRAG REDUCTION IN PRACTICAL SCRAMJET CONFIGURATIONS

Chan, W. Y. K. , Mee, D. J. , Smart, M. K. , Turner, J. C. , Stalker, R. J.
Centre for Hypersonics, School of Mechanical & Mining Engineering,
The University of Queensland, QLD 4072, Australia

Keywords: *boundary layer combustion, turbulent skin friction drag, drag reduction, flow non-uniformity, supersonic combustion*

Abstract

A key issue that can affect the implementation of boundary layer combustion for viscous drag reduction in scramjet combustors is the potential of non-uniform flow entering the combustor from the inlet. Experiments were conducted in the T4 Stalker tube to study the effects of these flow non-uniformities on boundary layer combustion in a circular constant-area combustor. A Rectangular-to-Elliptical-Shape-Transition (REST) inlet, typical of the type of inlets proposed for self-starting scramjet inlets, was attached upstream of the combustor in the current experiments. A numerical simulation of the flow through the REST inlet showed that the inlet generated a non-uniform outflow that had shock and expansion waves. The skin friction drag measured on the inner surface of the combustor indicated a reduction in skin friction drag of 30% when hydrogen burns in the boundary layer. More importantly, these experiments showed that a significant level of skin friction reduction due to boundary layer combustion was still achievable even in the presence of flow non-uniformities from the REST inlet.

Nomenclature

A_{cc}	Internal surface area of combustion chamber
c_p	Pressure coefficient
c_d	Drag coefficient
H_s	Nozzle supply enthalpy
M_∞	Freestream Mach number
p	Static pressure
p_∞	Freestream static pressure
T_∞	Freestream static temperature
u_∞	Freestream velocity
x	Distance from leading edge of REST inlet
γ_∞	Ratio of specific heats
ρ_∞	Freestream static density

1 Introduction

Boundary layer combustion is a method proposed in the Centre for Hypersonics at The University of Queensland in 2000 for the reduction of viscous drag in hypervelocity applications [8]. This technique involves the injection and, significantly, combustion of hydrogen in supersonic turbulent boundary layers. The combustion of hydrogen releases heat energy, which in turn, increases the temperatures in the boundary layers. This then reduces the boundary layer densities and Reynolds stresses, hence reducing the turbulent skin friction drag [3].

When fuel burns in the mainstream of a constant-area scramjet combustor, the skin friction drag is similar to that when fuel injection is not present [7, 32]. However, if fuel burns in the boundary layer instead of the mainstream, the heat released increases the displacement thickness of the boundary layer. This compresses the flow outside the boundary layer, hence decreasing its Mach number and increasing its temperature and pressure. The resulting skin friction

coefficient that would be obtained for the new freestream conditions could be up to double that for no fuel injection [11]. Instead of an increase in the level of skin friction drag, past experiments with boundary layer combustion [8, 11, 12, 30] have shown that measured skin friction coefficients can be up to 40% lesser than those measured when no fuel is injected. The effectiveness of this technique in reducing viscous drag is further confirmed by numerical simulations [4, 14, 29] and also by Stalker's theoretical analysis of the boundary layer combustion phenomena [28].

Although the results so far have shown that boundary layer combustion can be used to reduce turbulent skin friction drag and hence increase the net thrust output, a question that remains unanswered is whether this new technology can be implemented in combustion chambers of operational scramjet-powered vehicles. One key issue that can affect the implementation of the boundary layer combustion technique in proposed operational scramjet configurations is the potential of non-uniform flow entering the combustion chamber from the inlet. The presence of vortical structures due to fuel injection and shock and expansion waves may lead to the disruption of the wall fuel layer. The question is then whether such disruptions will drive the combustion away from the wall layer and remove the benefits of boundary layer combustion.

Past experiments conducted to investigate the boundary layer combustion technique have been done in a quasi direct-connect manner. For these experiments, non-uniformities in the flow were relatively small. In the current experiments, a Rectangular-to-Elliptical-Shape-Transition (REST) inlet [21] is coupled to a circular combustion chamber designed for implementing the boundary layer combustion technique. REST inlets are typical of the type of inlets proposed for self-starting scramjet inlets [5] - they have rectangular capture shapes which allow for easy mounting onto the airframe of vehicles, an elliptical/circular combustor which is structurally superior in comparison with rectangular ones, a fixed geometry and no boundary layer bleeds which results in greater scramjet system simplicity, and good self-starting capabilities [22]. REST inlets have also been shown to operate well at off-design conditions [23, 24, 31].

2 Experiments

2.1 Test Facility & Test Conditions

All experiments were conducted in the T4 Stalker tube at The University of Queensland. An axisymmetric contoured nozzle designed to produce a uniform test flow with a nominal Mach number of 6 was used. The test gases used for these experiments were air and nitrogen. The main purpose of using nitrogen as the test gas was to suppress combustion when fuel was injected. When combustion occurs, effects on pressure and drag forces can be brought about by both fuel injection and combustion. The suppression of combustion can aid in distinguishing the effects of fuel injection from those of combustion. The nominal freestream conditions for the shots with air as the test gas are given in Table 1. These freestream properties were estimated using the non-equilibrium nozzle flow code NENZF [15], which uses the nozzle supply conditions provided by ESTCj. ESTCj is a modified version of ESTC [17] which uses the CEA [16] chemistry database to estimate the nozzle supply conditions.

Table 1 Nominal test conditions

Flow parameter	Value	Shot-to-shot variation	Uncertainty
H_s	4.78 MJ/kg	±0.6%	±8%
p_∞	9.58 kPa	+3%	±12%
T_∞	563 K	±0.5%	±8%
ρ_∞	0.0592 kg/m^3	+4%	±11%
u_∞	2920 m/s	±3%	±3%
M_∞	6.2	±0.2%	±2%
γ_∞	1.38	<0.1%	

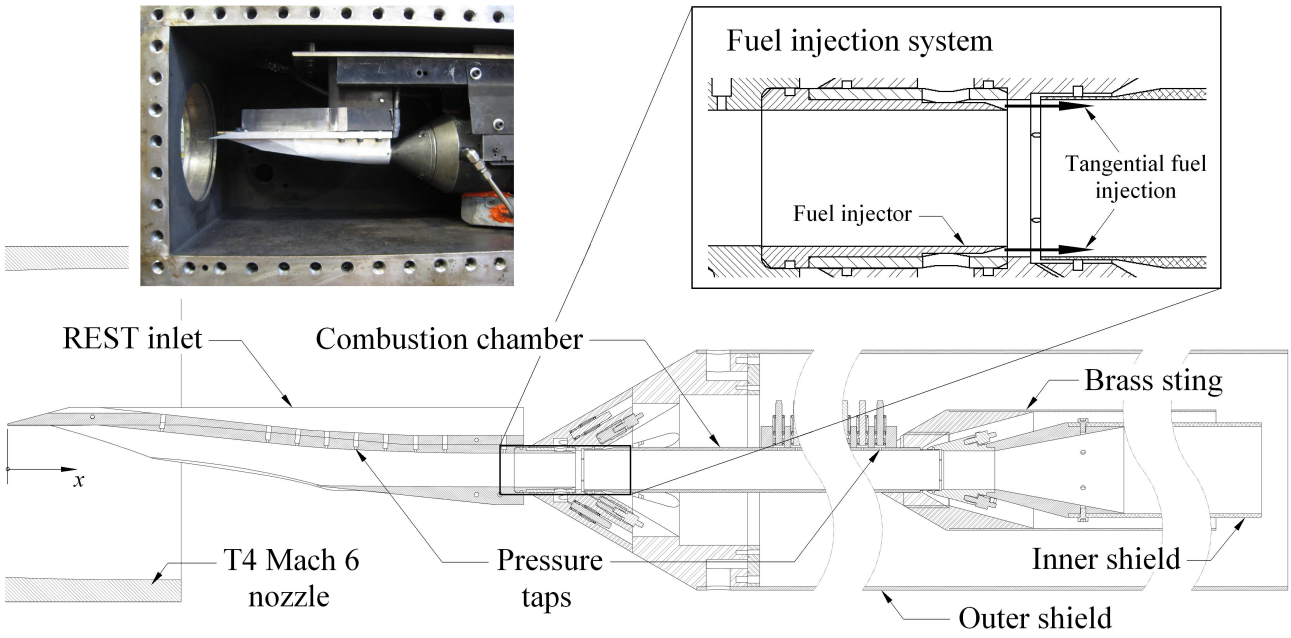

Fig. 1 Schematic of experimental setup

2.2 Experimental Model

The experimental setup, shown in Figure 1, consists of three major components - an aluminium REST inlet, a brass fuel injector and a circular aluminium combustion chamber. The combustion chamber, which is similar to that used in the experiments of Kirchhartz [11], is attached to a stress wave force balance for the measurement of net skin friction drag.

In order to directly compare the current experiments with those of Kirchhartz [11] to examine the influence of flow non-uniformities, the REST inlet was designed to produce combustor entry conditions similar to those obtained for the direct-connect inlet in Kirchhartz's experiments. The 440-mm long REST inlet has a 100-mm wide frontal capture area of 2.5×10^{-3} m^2 that contracts to a circular exit area of 6.5×10^{-4} m^2, which equates to a total geometric contraction ratio of 3.84. All leading edges have a 0.5 mm radius bluntness. The centreline of the upper (bodyside) surface of this inlet was instrumented with nine Kulite XTEL-100-190M pressure transducers at x = 130 mm, 220 mm, 245 mm, 269 mm, 294 mm, 319 mm, 345 mm, 370 mm and 420 mm from the leading edge (see Figure 1). For these experiments, the inlet was positioned in the test section of the test facility such that the entire capture area sat within the uniform core flow region of the T4 Mach 6 nozzle [19].

A brass fuel injector was connected to the end of the REST inlet. Shown in detail in Figure 1, the injector delivered fuel through an annular slot which had a throat area of 6.65×10^{-5} m^2 and an exit area of 2.14×10^{-4} m^2. Hydrogen was supplied to this injector from a Ludweig tube fuel delivery system. The use of a Ludweig tube fuel delivery system ensured that a near constant fuel flow rate was available during the test time of these experiments [6]. A typical fuel mass flow rate for the current experiments is 0.012 kg/s, which corresponds to a fuel equivalence ratio of approximately 1.0.

The 500-mm long combustion chamber of 33.2 mm internal diameter was instrumented with 20 PCB 112A pressure transducers. The first transducer was located 160 mm from the fuel injection plane and subsequent transducers were located 15 mm apart from one another. The combustor was attached to a 2430-mm long brass sting that was instrumented with a piezoelectric

film strain gauge [26] located 238 mm from the leading edge of the sting. The gauge on the brass sting was used to measure the stress waves generated when skin friction drag acts on the internal surface of the combustion chamber. The measured strain signals can then be deconvolved with an impulse response to reproduce the actual drag force acting on the combustion chamber [18]. The impulse response was obtained from calibrations in which the front edge of the combustor was struck with an instrumented impact hammer. More details about the measurement of forces by the stress wave force balance technique are given in References [20], [25], [27] and [33]. As only the skin friction drag on the internal surface of the combustion chamber was to be measured, the remaining parts of the combustion chamber and brass sting assembly were shielded from the test flow. This was done via the outer and inner shields shown in Figure 1. Due to design limitations, the front edge, rear edge and rear cavity surfaces of the combustor-sting assembly can still be exposed to some pressures when the test flow arrives. To ensure that only skin friction drag acting on the internal surface of the combustion chamber was extracted, these pressures were measured and the forces due to these pressures were accounted for in the drag measurements. The levels of corrections were typically less than 1% of the net skin friction drag for tests without fuel injection and 14% for tests in which combustion occurred.

2.3 Experimental Uncertainties

Shot-to-shot repeatability of the duct pressure coefficient for identical nominal freestream conditions was established to within $\pm 5\%$ for most measurement locations. The measurement uncertainty for the pressure coefficient was estimated to be within $\pm 14\%$. The experimental uncertainty for the measured forces was estimated to be $\pm 10\%$.

3 CFD simulation of the REST inlet

A CFD simulation of the flow in the REST inlet was performed using the VULCAN code [34]. VULCAN is a structured, finite-volume CFD code that solves the Favre-averaged Navier-Stokes equations. Inviscid fluxes were calculated using the low-dissipation flux splitting scheme of Edwards with Van Leer limiter, while viscous fluxes were evaluated using second-order central differences. Turbulence was modelled using the $k-\omega$ model of Wilcox [35] while the Reynolds stresses were modelled using the Boussinesq model. The boundary layer was assumed to be turbulent from the leading edge of the REST inlet. The use of wall functions with the turbulence model allowed the y^+ value of wall cells to be in the order of 60. The inlet was modelled using a grid that had 2056300 cells. The walls of the inlet were assumed to have a constant temperature of 300 K. Air, which was assumed to be a mixture of thermally perfect gases, was used as the inflow gas in the simulation. This inflow was assumed to have a turbulence intensity of 0.01 and a turbulent viscosity ratio of 0.1.

4 Results & Discussion

The two main types of data extracted from these experiments are pressures and forces. A typical static pressure trace from a transducer in the REST inlet is shown in Figure 2. The test time is taken to start when the flow has established in the nozzle and experimental model. The start up time for the shock tunnel nozzle used in these experiments is typically 0.8 ms. It is assumed that three flow lengths is required for the flow to be fully established [10] in the current model - this corresponds to a flow establishment time of about 1.0 ms for this test condition. The end of test time is determined by either when the drop by more than 5% in nozzle-supply pressure or when 10% driver gas flow contamination occurs [1]. The pressure distributions are presented in the form of pressure coefficients (see Equation 1).

$$c_p = \frac{p - p_\infty}{\frac{1}{2}\rho_\infty u_\infty^2} \tag{1}$$

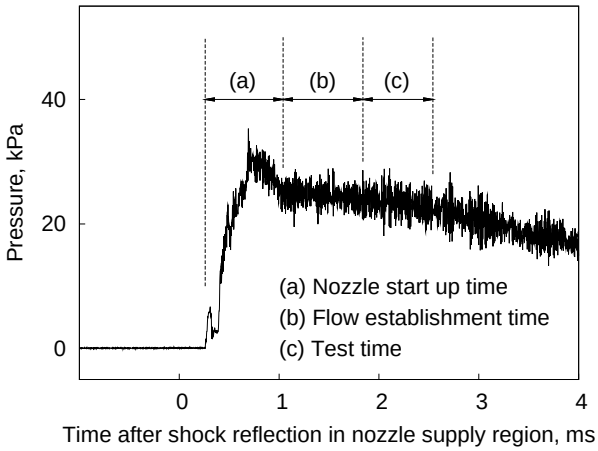

Fig. 2 Typical pressure trace from shot 10563

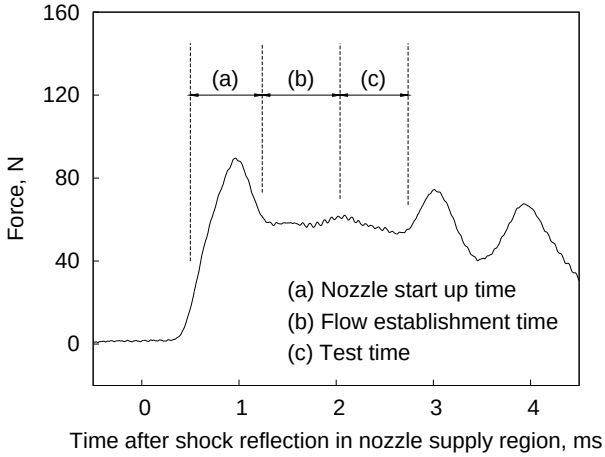

Fig. 3 Typical force trace from shot 10563

Figure 3 shows a typical force trace that has been deconvolved from a strain signal measured via the thin film gauge. Note that this trace had been passed through a 250-μs moving average filter. The sharp rise and drop in the force signal from 0.5 ms to 1.3 ms is associated with the nozzle starting pressures. A similarly shaped signal can be seen in the pressure traces (see Figure 2). The other unsteady rises and drops after 2.8 ms are attributed to the edges of the combustion chamber hitting the other parts of the model. Note that these occur after the steady test flow. The force data are presented as drag coefficients (see Equation 2).

$$c_d = \frac{D}{\frac{1}{2}\rho_\infty u_\infty^2 A_{cc}} \tag{2}$$

4.1 REST inlet pressure measurements

The pressures measured in the inlet confirmed that the flow through the inlet had started and established during the tests. Figure 4 shows a comparison between experimentally measured and numerically simulated static pressures along the centreline of the bodyside surface of the REST inlet. The pressure coefficients for tests without fuel injection, tests with fuel injection into air and tests with fuel injection into nitrogen are labelled "*Fuel-off*", "*Fuel-on*" and "*Fuel-N2*" respectively. The numerical simulation was completed for the *fuel-off* test using VULCAN, as described in Section 3. The numerical results generally match the experiments well, except for a discrepancy at $x = 0.37$ m. The blunted leading edges of the REST inlet were not modelled in the simulation. This may account for a difference seen between the numerical and experimental results for the location of the shock which impinges near $x = 0.4$ m (see Figure 4).

A goal of the design of the REST inlet was to produce similar conditions at entry to the combustor as those obtained in Kirchhartz's experiments. Figures 5, 6 and 7 show the freestream conditions taken at 45 mm upstream of the fuel injection plane for the current experiments and for Kirchhartz's experiments. The freestream conditions for the current experiments were taken from the CFD simulation described in Section 3 whereas those for Kirchhartz's experiments were extracted from the CFD simulation performed by Kirchhartz [11]. It can be observed from these plots that similar conditions have been achieved. The mismatch in certain areas, for example the drop in pressure due to expansion waves seen in Figure 7, is to be expected since the REST inlet generated a more non-uniform flow. Figures 5 and 6 also show that thicker and hotter boundary layers, which are favourable for the boundary layer combustion technique [13], are present on the bodyside surface of the inlet. Figure 6 shows that boundary layer temperatures on the lower surface of the inlet are lower than those of Kirch-

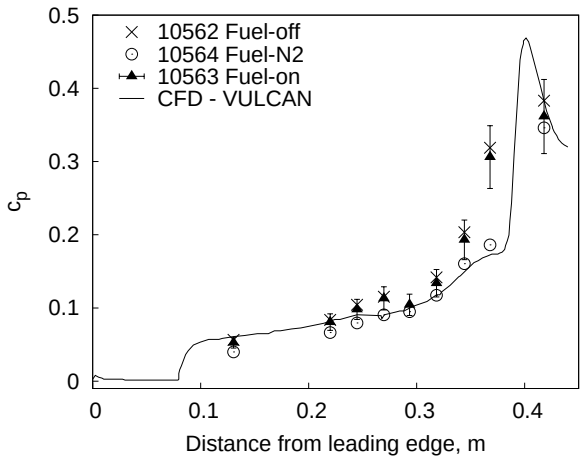

Fig. 4 Development of static pressure along the centreline of the bodyside surface of the REST inlet

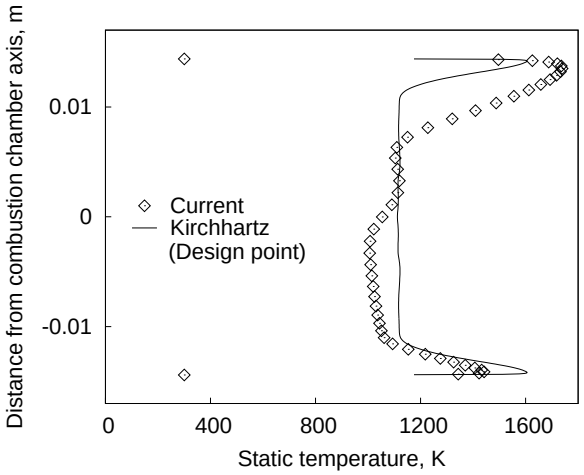

Fig. 6 Comparison of freestream static temperature at 45 mm upstream of the fuel injection plane

hartz's. The ignition temperature for a hydrogen-air mixture at 100 kPa with an ignition length of 100 mm is approximately 1140 K [9]. Since the peak boundary layer temperature of 1440 K (see Figure 6) is higher than the ignition temperature, the ignition of hydrogen should not be significantly affected by the reduced boundary layer temperatures on the lower surface of the REST inlet.

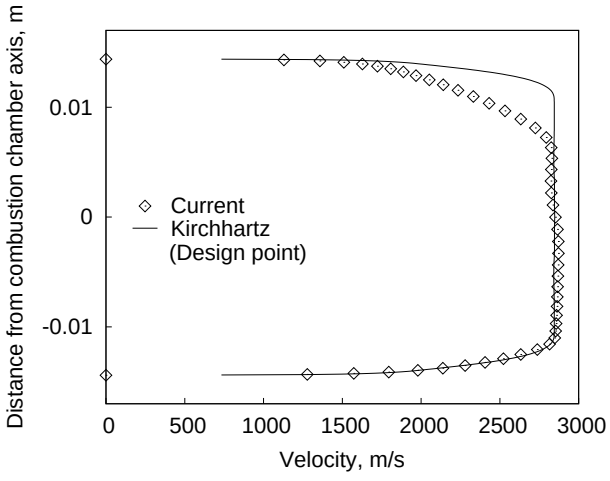

Fig. 5 Comparison of freestream velocity at 45 mm upstream of the fuel injection plane

4.2 Combustion chamber pressure measurements

Figure 8 shows the experimentally measured static pressure along the combustion chamber for *fuel-off*, *fuel-on* and *fuel-N2* tests. As expected, there are no discernable differences in the static pressure distribution between *fuel-off* and *fuel-N2* tests since no combustion occurs. However, when fuel is injected and combustion does occur, a significant pressure rise is obtained. One question that then arises is whether the fuel is burning in the mainstream or in the boundary layer. This is addressed in Section 4.3 when examining the skin friction drag.

The ignition of hydrogen can be seen in the pressure distribution at about 230 mm downstream of the fuel injection plane in Figure 8. It is postulated that the ignition of the fuel may be associated with a shock impingement, since the ignition location coincides with a shock impingement location seen in both *fuel-off* and *fuel-N2* tests. The difference in pressures between the *fuel-on* and *fuel-off* tests at 150 mm downstream of the fuel injection plane suggests that a small level of combustion could be occurring upstream of that location.

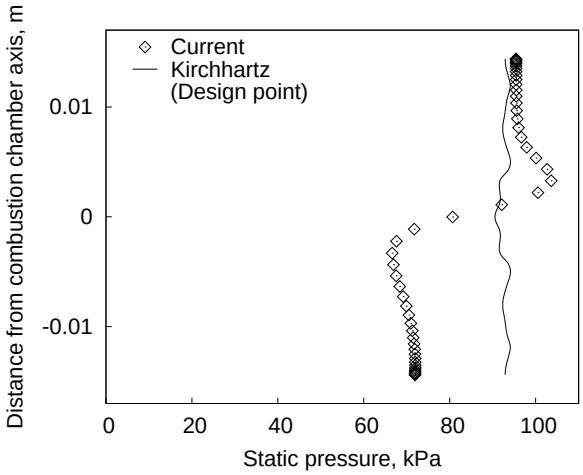

Fig. 7 Comparison of freestream static pressure at 45 mm upstream of the fuel injection plane

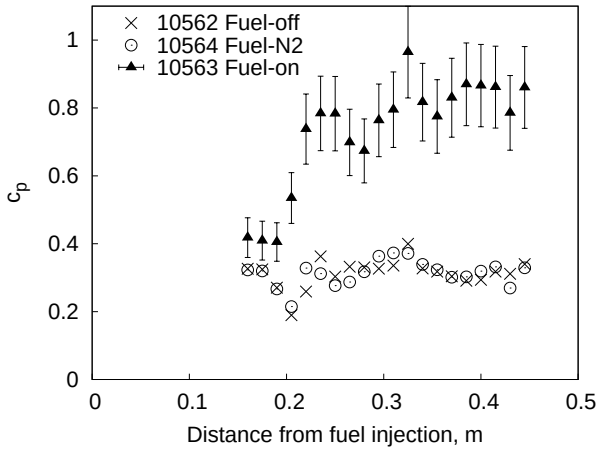

Fig. 8 Pressure coefficient along combustion chamber

4.3 Combustion chamber skin friction drag measurements

Figure 9 shows the experimentally derived drag force acting on the internal walls of the combustion chamber for *fuel-off*, *fuel-on* and *fuel-N2* tests. Note that the drag coefficients in Kirchhartz's data set are lower than those in the current data set. The shock tunnel nozzle used in the current experiments produced a Mach 6.2 flow whereas the nozzle used in Kirchhartz's direct-connect experiments produced a Mach 4.5 flow. The use of a larger ρu^2 value for the Mach 4 nozzle when normalising the drag data causes the drag coefficient to be lower than that when the ρu^2 value for the Mach 6 nozzle in the current experiments is used.

Both sets of experiments show a reduction in skin friction drag when fuel is injected into nitrogen test gas. This drag reduction is brought about by the commonly known film-cooling phenomena [2]. More importantly, a further reduction in skin friction drag can be observed when the fuel burns. It has been shown in the experiments by Goyne [7] and Tanno [32] that skin friction drag in a constant-area combustor is essentially unchanged when fuel burns in the mainstream. The reduction in drag coefficient when combustion occurs (see Figure 9) therefore indicates that the fuel is indeed burning in the boundary layer and not just in the mainstream.

For the current experiments, the drag coefficient for *fuel-N2* tests is 84% of that for *fuel-off* tests while the drag coefficient for *fuel-on* tests is 71% of that for *fuel-off* tests. For Kirchhartz's experiments, the drag coefficient for *fuel-N2* tests is 80% of that for *fuel-off* tests while the drag coefficient for *fuel-on* tests is 65% of that for *fuel-off* tests. The skin friction drag reduction measured in the current experiments is 4% lower than that measured in Kirchhartz's experiments when combustion is suppressed with nitrogen test gas and 6% lower when combustion occurs. Note that these differences are within the experimental uncertainties. The slightly diminished levels in skin friction reduction may be associated with the flow non-uniformities from the REST inlet. Despite this, the important point to note from the current experiments is that a significant level of skin friction reduction due to boundary layer combustion is still achievable even in the presence of flow non-uniformities from the REST inlet.

5 Conclusion

These experiments show that a significant of level of skin friction reduction is achievable when hydrogen burns in the boundary layer. More importantly, these experiments also show that flow non-uniformities generated from a practical scramjet inlet do not significantly diminish the level of

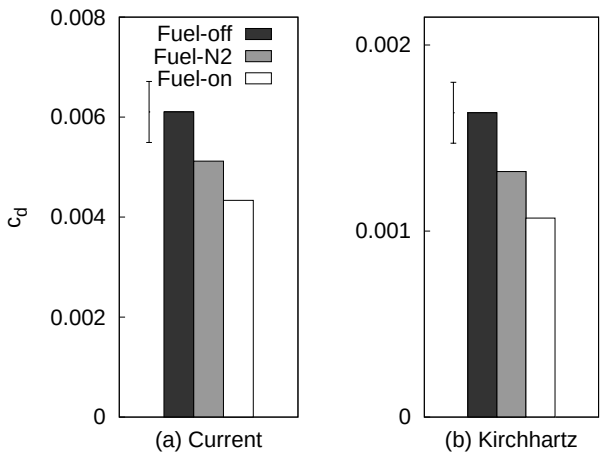

Fig. 9 Skin friction drag acting on the internal walls of combustion chamber for (a) current experiments and (b) Kirchhartz's experiments [11]

skin friction reduction achievable by the boundary layer combustion technique. Slightly diminished levels of skin friction reduction were observed in the current experiments in comparison to those obtained at similar conditions for an inflow without flow distortions. Numerical simulations need to be conducted to ascertain if flow non-uniformities from the REST inlet are the cause for this.

Acknowledgements

The authors gratefully acknowledge support for this project from the Australian Research Council under grant DP0665016. The authors would also like to thank Dylan Wise, Luke Doherty and Andrew Ridings for operating the shock tunnel during these experiments, Grant Tayles and Keith Hitchcock for fabricating parts of the experimental model, and Dr Rainer Kirchhartz for his insightful comments throughout these experiments.

References

[1] Boyce R. R, Takahashi M, and Stalker R. J. Mass spectrometric measurements of driver gas arrival in the T4 free-piston shock-tunnel. *Shock Waves*, Vol. 14, No 5/6, pp 371–378, 2005.

[2] Cary Jr A. M and Hefner J. N. Film-cooling effectiveness and skin friction in hypersonic turbulent flow. *AIAA Journal*, Vol. 10, No 3, pp 1188–1193, September 1972.

[3] Denman A. W. *Large-eddy simulation of compressible turbulent boundary layers with heat addition*. PhD thesis, The University of Queensland, Queensland, Australia, 2007.

[4] Denman A. W, Jacobs P. A, and Mee D. J. Compressible turbulent flow with boundary-layer heat addition. *Proc 43rd AIAA Aerospace Sciences Meeting and Exhibit*, No AIAA 2005-1097, Reno, Nevada, USA, 10-13 January 2005. American Institute of Aeronautics and Astronautics Inc.

[5] Eggers T, Silvester T. B, Paull A, and Smart M. K. Aerodynamic design of hypersonic re-entry flight HIFiRE 7. *Proc 16th AIAA/DLR/DGLR International Space Planes and Hypersonic Systems and Technologies Conference*, No AIAA 2009-7256, Bremen, Germany, 19-22 October 2009. American Institute of Aeronautics and Astronautics Inc.

[6] Gangurde D. Y, Mee D. J, and Jacobs P. A. Numerical simulation of a Ludwieg-tube fuel delivery system for scramjet experiments in shock tunnels. *Proc 16th Australasian Fluid Mechanics Conference*, Gold Coast, Queensland, Australia, December 2007. School of Engineering, The University of Queensland.

[7] Goyne C. P, Stalker R. J, and Paull A. Shock-tunnel skin-friction measurement in a supersonic combustor. *Journal of Propulsion and Power*, Vol. 15, No 5, pp 699–705, September-October 1999.

[8] Goyne C. P, Stalker R. J, Paull A, and Brescianini C. P. Hypervelocity skin-friction reduction by boundary-layer combustion of hydrogen. *Journal of Spacecraft and Rockets*, Vol. 37, No 6, pp 740–746, November 2000.

[9] Huber P. W, Schexnayder C. J. J, and McClinton C. R. Criteria for self-ignition of supersonic hydrogen-air mixtures. NASA Technical Paper NASA-TP-1457, NASA, August 1979.

[10] Jacobs P. A, Rogers R. C, Weidner E. H, and Bittner R. D. Flow establishment in a generic scramjet combustor. *Journal of Propulsion and Power*, Vol. 8, No 4, pp 890–899, July-August 1992.

[11] Kirchhartz R. M. *Upstream wall layer effects*

on drag reduction with boundary layer combustion. PhD thesis, The University of Queensland, Queensland, Australia, 2010.

[12] Kirchhartz R. M, Mee D. J, and Stalker R. J. Skin friction drag with boundary layer combustion in a circular combustor. *Proc 15th AIAA International Space Planes and Hypersonic Systems and Technologies Conference*, No AIAA 2008-2589, Dayton, Ohio, USA, 28 April - 1 May 2008. American Institute of Aeronautics and Astronautics Inc.

[13] Kirchhartz R. M, Mee D. J, Stalker R. J, Jacobs P. A, and Smart M. K. Supersonic boundary-layer combustion: Effects of upstream entropy and shear-layer thickness. *Journal of Propulsion and Power*, Vol. 26, No 1, pp 57–66, 2010.

[14] Levin V. A and Larin O. B. Skin-friction reduction by energy addition into a turbulent boundary layer. *Proc 41st AIAA Aerospace Sciences Meeting and Exhibit*, No AIAA 2003-0036, Reno, Nevada, USA, 6-9 January 2003. American Institute of Aeronautics and Astronautics Inc.

[15] Lordi J. A, Mates R. E, and Moselle J. R. Computer program for the numerical simulation of non-equilibrium expansions of reaction gas mixtures. NASA Contractor Report NASA-CR-472, Cornell Aeronautical Laboratory, Inc., Buffalo, NY, 1966.

[16] McBride B. J, Zehe M. J, and Gordon S. NASA glenn coefficients for calculating thermodynamic properties of individual species. NASA Technical Paper NASA-TP-2002-211556, NASA John H. Glenn Research Center at Lewis Field, Cleveland, Ohio, September 2002.

[17] McIntosh M. K. Computer program for the numerical calculation of frozen and equilibrium conditions in shock tunnels. Departmental Report, Department of Physics, Australian National University, Canberra, Australia, 1968.

[18] Mee D. J. Dynamic calibration of force balances for impulse hypersonic facilities. *Shock Waves*, Vol. 12, pp 443–455, 2003.

[19] Overton S and Mee D. J. T4's M5 and M8 nozzle pitot rake survey. *Proc The 4th International Workshop on Shock Tube Technology Proceedings*, Brisbane, Australia, 20-23 September 1994.

[20] Sanderson S and Simmons J. Drag balance for hypervelocity impulse facilities. *AIAA Journal*, Vol. 29, No 12, pp 2185–2191, December 1991.

[21] Smart M. K. Design of three-dimensional hypersonic inlets with rectangular-to-elliptical shape transition. *Journal of Propulsion and Power*, Vol. 15, No 3, pp 408–416, May-Jun 1999.

[22] Smart M. K. Experimental testing of a hypersonic inlet with rectangular-to-elliptical shape transition. *Journal of Propulsion and Power*, Vol. 17, No 2, pp 276–283, March-April 2001.

[23] Smart M. K and Ruf E. G. Free-jet testing of a REST scramjet at off-design conditions. *Proc Collection of Technical Papers - 25th AIAA Aerodynamic Measurement Technology and Ground Testing Conference*, San Francisco, California, USA, June 2006. American Institute of Aeronautics and Astronautics Inc.

[24] Smart M. K and Trexler C. A. Mach 4 performance of hypersonic inlet with rectangular-to-elliptical shape transition. *Journal of Propulsion and Power*, Vol. 20, No 2, pp 288–293, March-April 2004.

[25] Smith A. L and Mee D. J. Drag measurements in a hypervelocity expansion tube. *Shock Waves*, Vol. 6, pp 161–166, 1996.

[26] Smith A. L and Mee D. J. Dynamic strain measurement using piezoelectric polymer film. *Journal of Strain Analysis*, Vol. 31, No 6, pp 463–465, 1996.

[27] Smith A. L, Mee D. J, Daniel W. J. T, and Shimoda T. Design, modelling and analysis of a six component force balance for hypervelocity wind tunnel testing. *Computers and Structures*, Vol. 79, pp 1077–1088, 2001.

[28] Stalker R. J. Control of hypersonic turbulent skin friction by boundary-layer combustion of hydrogen. *Journal of Spacecraft and Rockets*, Vol. 42, No 4, pp 577–587, July-August 2005.

[29] Stephensen D. *Controlling skin friction by boundary layer combustion*. Bachelor of engineering (Honours) thesis, The University of Queensland, Queensland, Australia, November 2002.

[30] Suraweera M. V. *Reduction of skin friction drag in hypersonic flow by boundary layer*. PhD the-

sis, The University of Queensland, Queensland, Australia, 2006.

[31] Suraweera M. V and Smart M. K. Shock-tunnel experiments with a Mach 12 Rectangular-to-Elliptical Shape-Transition scramjet at off-design conditions. *Journal of Propulsion and Power*, Vol. 25, No 3, pp 555–564, May-June 2009.

[32] Tanno H, Paull A, and Stalker R. J. Skin-friction measurements in a supersonic combustor with crossflow fuel injection. *Journal of Propulsion and Power*, Vol. 17, No 6, pp 1333–1338, November-December 2001.

[33] Tuttle S. L, Mee D. J, and Simmons J. M. Drag measurements at Mach 5 using a stress wave force balance. *Experiments in Fluids*, Vol. 19, No 5, pp 336–341, September 1995.

[34] White J. A and Morrison J. H. A pseudo-temporal multi-grid relaxation scheme for solving the parabolized Navier-Stokes equations. *Proc 14th AIAA Computational Fluid Dynamics Conference*, No AIAA Paper 99-3360. American Institute of Aeronautics and Astronautics Inc., 28 June - 1 July 1999.

[35] Wilcox D. C. *Turbulence modelling for CFD*. 3rd edition, DCW Industries, Inc, California, USA, November 2006.

Copyright Statement